J Arid Land (2023) 15(10): 1196–1215
https://doi.org/10.1007/s40333-023-0109-1

Science Press Springer-Verlag

Spatial distribution and ecological risk of heavy metals and their source apportionment in soils from a typical mining area, Inner Mongolia, China

XIE Shicheng[1,2,3], LAN Tian[4], XING An[1,2,3], CHEN Chen[1,2,3], MENG Chang[1,2,3], WANG Shuiping[1,2,3], XU Mingming[1,2,3], HONG Mei[1,2,3*]

[1] Inner Mongolia Agricultural University, Hohhot 010018, China;
[2] Inner Mongolia Key Laboratory of Soil Quality and Nutrient Resources, Hohhot 010018, China;
[3] Key Laboratory of Agricultural Ecological Security and Green Development at Universities of Inner Mongolia Autonomous Region, Hohhot 010018, China;
[4] School of Environment, Tsinghua University, Beijing 100084, China

Abstract: Determining the distributions and sources of heavy metals in soils and assessing ecological risks are fundamental tasks in the control and management of pollution in mining areas. In this study, we selected 244 sampling sites around a typical lead (Pb) and zinc (Zn) mining area in eastern Inner Mongolia Autonomous Region of China and measured the content of six heavy metals, including cuprum (Cu), Zn, Pb, arsenic (As), cadmium (Cd), and chromium (Cr). The ecological risk of heavy metals was comprehensively evaluated using the Geo-accumulation index, Nemerow general pollution index, and potential ecological risk index. The heavy metals were traced using correlation analysis and principal component analysis. The results showed that the highest content of heavy metals was found in 0–5 cm soil layer in the study area. The average content of Zn, As, Pb, Cu, Cr, and Cd was 670, 424, 235, 162, 94, and 4 mg/kg, respectively, all exceeding the risk screening value of agricultural soil in China. The areas with high content of soil heavy metals were mainly distributed near the tailings pond. The study area was affected by a combination of multiple heavy metals, with Cd and As reaching severe pollution levels. The three pathways of exposure for carcinogenic and noncarcinogenic risks were ranked as inhalation>oral ingestion>dermal absorption. The heavy metals in the study area posed certain hazards to human health. Specifically, oral ingestion of these heavy metals carried carcinogenic risks for both children and adults, as well as noncarcinogenic risks for children. There were differences in the sources of different heavy metals. The tailings pond had a large impact on the accumulation of Cd, Zn, and Pb. The source of Cr was the soil parent material, the source of As was mainly the soil matrix, and the source of Cu was mainly the nearby Cu ore. The purpose of this study is to more accurately understand the extent, scope, and source of heavy metals pollution near a typical mining area, providing effective help to solve the problem of heavy metals pollution.

Keywords: heavy metal; ecological risk; Geo-accumulation index; Nemerow general pollution index; tailings pond; mining area

Citation: XIE Shicheng, LAN Tian, XING An, CHEN Chen, MENG Chang, WANG Shuiping, XU Mingming, HONG Mei. 2023. Spatial distribution and ecological risk of heavy metals and their source apportionment in soils from a typical mining area, Inner Mongolia, China. Journal of Arid Land, 15(10): 1196–1215. https://doi.org/10.1007/s40333-023-0109-1

*Corresponding author: HONG Mei (E-mail: nmczhm1970@126.com)
Received 2023-03-20; revised 2023-08-03; accepted 2023-08-28

1 Introduction

The production of smelted lead (Pb), cuprum (Cu), and zinc (Zn) in China accounted for 50.5% of the global total production in 2018 (Shi et al., 2019). Chromium (Cr), Zn, Pb, arsenic (As), Cu, cadmium (Cd), and nickel (Ni) are listed as priority contaminants by the United States Environmental Protection Agency (USEPA) due to their low degradability, bioaccumulation, and toxicity (Muhammad, 2022). Among heavy metals, trace amounts of Cu, ferrum (Fe), and Zn are essential for human health. However, high concentrations of heavy metals can be toxic to humans and other organisms. Heavy metals, including Cd, Cr, Pb, and As, are toxic even in trace amounts and cause a variety of health problems. For example, Cd can cause high blood pressure, headaches, and osteoporosis, Cr poisoning can lead to liver and kidney dysfunction, and Pb can cause memory loss and anemia (Muhammad et al., 2021; Sehrish et al., 2021; Din et al., 2022). Mining activities are considered to be one of the main causes of heavy metals pollution in soil (Liu et al., 2020). The tailings pond is exposed to the natural environment over a long time and poses a serious threat to the entire ecosystem (Du et al., 2020; Wei et al., 2020). Heavy metals are not easily degradable and can accumulate in human body through the food chain and seriously endanger human health (Wang et al., 2016; Sun et al., 2019).

Targeted remediation strategies can be developed by conducting ecological risk assessments and tracing heavy metals. Many researchers have used indices or models, such as the enrichment factor index, Nemerow general pollution index (P_N), potential ecological risk index (RI), and human health risk assessment, to simulate soil heavy metals pollution and to study the effects of soil physical-chemical properties on the risk of soil heavy metals pollution (Liu et al., 2022). Cheng et al. (2018) used the P_N and RI to investigate soil heavy metals pollution in a Zn and Pb mining region in Yunnan Province of China, and found that 95% of the local soil is heavily contaminated with As. A study conducted by Chun et al. (2021) using a semi-variance-based model showed that the heavy metals content gradually decreased with increasing distance from the tailings pond in the Baiyinhua mining area of Inner Mongolia Autonomous Region, China. Yang et al. (2022) found that soil pH, organic matter, and cation exchange are important factors driving the transformation of soil heavy metals forms.

The hazard of heavy metals depends on the total amount, distribution, chemical form, and transport and transformation in the environment as well as biological toxicity. Based on the accumulation patterns of heavy metals, ecological risk assessment is conducted to explore the impact of heavy metals toxicity on human health (Li et al., 2003). Zhou et al. (2015) and Sun et al. (2017) evaluated heavy metals pollution in mining-concentrated areas and the western mining areas of Inner Mongolia, respectively; they found that nonferrous metal exploration area is dominated by slight ecological risk, but the total carcinogenic risk exceeds the acceptable range for humans. In addition, insufficient knowledge of the mobility and biological effectiveness of heavy metals also affects the risk evaluation of the surrounding ecological environment (Dong et al., 2019).

Inner Mongolia has huge mineral reserves, which is of great significance to the arrangement of mineral resources in China (Yang et al., 2022). Due to the fact that most of the mineral resources in Inner Mongolia are located in grasslands ecosystem with a weak resistance to disturbance, mining activities can lead to a great threat to the ecosystem. Ore mining, raw material processing and transportation, and tailings accumulation can cause significant soil contamination (Wang et al., 2018). Gao et al. (2017) found that the content of Pb, Ni, and Zn in the soil of a gold (Au) mining area in Xilinhot City, Inner Mongolia, is much higher than local background value. The result of pollution risk assessment revealed that most of the soil around a nonferrous metal mining area in Chifeng City, Inner Mongolia, is at moderate or heavy pollution levels, with large risk indices for As and Cd (Hu et al., 2018).

An extreme lack of soil contamination assessment work in the tailings pond has affected local ecological remediation measures. In this study, we analyzed the pollution of Cu, Zn, Pb, As, Cr, and Cd at 0–20 cm soil depth in a typical Pb and Zn mining area. The spatial

distribution characteristics of heavy metals in the mining area were analyzed, and the pollution assessment and source analysis of heavy metals were conducted. This study will contribute to a more accurate understanding of the level and extent of heavy metals pollution, identify the source of heavy metals, and develop precise, economical, and efficient remediation measures.

2 Materials and methods

2.1 Study area

The study area (43°20′–43°45′N, 117°54′–118°21′E) is located in a typical Pb and Zn mining area of Linxi County in Chifeng City, Inner Mongolia Autonomous Region of China (Fig. 1). The area is topographically mountainous with an average elevation of approximately 747 m a.s.l., and the terrain is generally high in the northeast and low in the southwest. The climate type is semiarid continental monsoon with low precipitation of approximately 330–360 mm. The dominant wind direction is northwest, and the annual average temperature is 5.8°C. The mining area is approximately 1.50 km^2, and the tailings pond covers an area of 0.15 km^2.

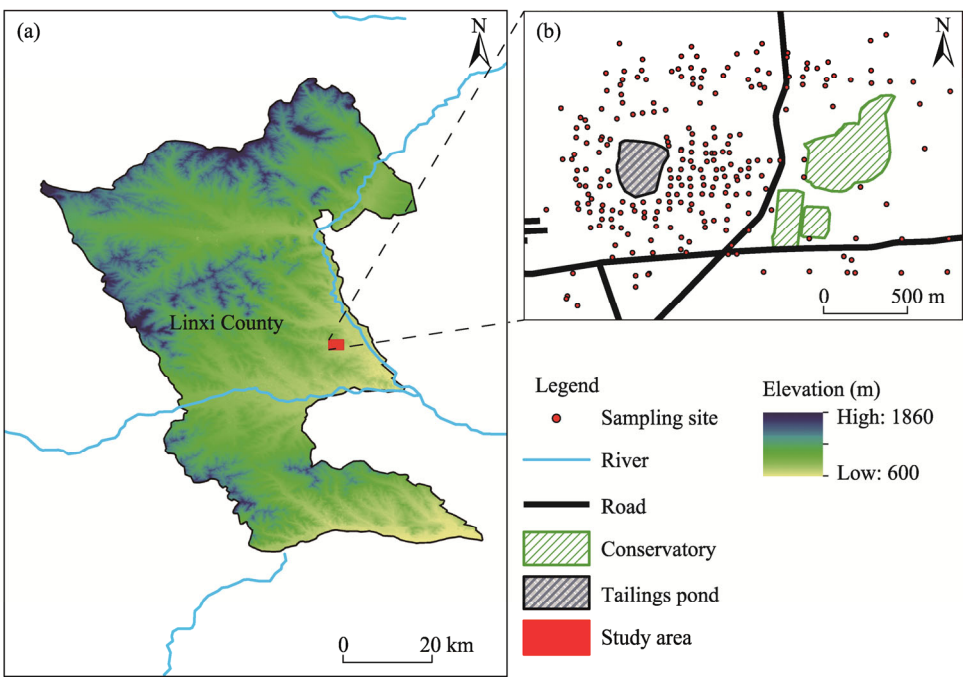

Fig. 1 Location of the study area (a) and spatial distribution of sampling sites (b)

2.2 Sample collection and analysis

According to field research, topography, and wind direction, we selected the sampling sites within 4.00 km^2 around the tailings pond, which are mainly distributed in farmland and woodland. We used Global Position System (GPS) to precisely determine the coordinates of each sampling site during soil sample collection. With the tailings pond as the research center and the satellite images as the basis, we set a 50 m×50 m grid in a 2 km×2 km area around the tailings pond for sampling. Samples were collected from the top layer (0–5, 5–10, and 10–20 cm) of agricultural soil, and five soil samples were collected at each sampling site along the diagonal for mixing. Approximately 1-kg soil samples were collected using the quadrat method and brought back to the laboratory. A total of 732 soil samples were collected, with each layer consisting of 244 samples. This study was conducted from October 2021 to March 2022. Soil samples were collected from 1 October to 8 October in 2021, and the experiment was conducted from October 2021 to March 2022.

The collected soil samples were sieved to remove foreign matter such as weeds and twigs. After natural drying, the soil samples were ground and passed through a 100 mesh nylon sieve. The content of heavy metals (including Pb, Zn, Cu, As, Cd, and Cr) in soil samples was determined by microwave digestion with the HNO_3-H_2SO_4-$HClO_4$-HF method and inductively coupled plasma mass spectrometry (iCAP RQplus ICP-MS, Thermo Scientific, Beijing, China). Three parallel samples were measured for each soil sample, and the recoveries of all elements after sample digestion ranged from 80% to 137%. Electrical conductivity (EC) was determined using the conductivity method, and pH was measured using a pH meter (STARTER 2100, OHAUS, Paramus, United States of America) with a ratio of soil to water of 1:5.

2.3 Assessment methods

The Geo-accumulation index (I_{geo}), P_N, and RI were used to evaluate the pollution of soil heavy metals.

2.3.1 Geo-accumulation index (I_{geo})

The I_{geo} is used to qualitatively assess the pollution level of individual heavy metals (Muller, 1969). It accounts for the influence of natural factors on background values, identifies the impact of anthropogenic activities on environment (Fei et al., 2019), and directly evaluates the pollution level of heavy metals through the change in actual heavy metals measurements relative to the environmental baseline values (Loska et al., 2004). Soil environmental quality—risk control standard for soil contamination of agricultural land (Ministry of Ecology and Environment of the People's Republic of China, 2018) was used as the baseline value for the soil pollution evaluation. I_{geo} is calculated as follows:

$$I_{geo} = \log_2 \frac{C_n}{1.5B_n}, \tag{1}$$

where C_n is the measured content of heavy metals (mg/kg); and B_n is the background value of heavy metals content in soil (mg/kg), referring to soil environmental quality–risk control standard for soil contamination of agricultural land quality (Ministry of Ecology and Environment of the People's Republic of China, 2018). The values of I_{geo} are classified into seven levels, including no pollution (I_{geo}<0), light pollution (0≤I_{geo}<1), partial moderate pollution (1≤I_{geo}<2), moderate pollution (2≤I_{geo}<3), partial heavy pollution (3≤I_{geo}<4), heavy pollution (4≤I_{geo}<5), and severe pollution (I_{geo}≥5).

2.3.2 Nemerow general pollution index (P_N)

The P_N is an evaluation method based on a single-factor index (Liu et al., 2019). It not only reflects the degree of regional pollution by heavy metals but also can be used to evaluate the soil quality or composite pollution of whole region (Li et al., 2021). The calculation formulas of P_N are as follows:

$$P_i = C_n / B_n, \tag{2}$$

$$P_N = \sqrt{\frac{P_{i(\text{ave})}^2 + P_{i(\text{max})}^2}{2}}, \tag{3}$$

where P_i is single-factor index; and $P_{i(\text{ave})}$ and $P_{i(\text{max})}$ are the average and maximum values of P_i, respectively. We classified the P_N into five levels: no pollution (P_N<1), light pollution (1≤P_N<2), moderate pollution (2≤P_N<3), heavy pollution (3≤P_N<5), and severe pollution (P_N≥5).

2.3.3 Potential ecological risk index (RI)

The RI is characterized by its ability to reflect biological effectiveness and spatial variation (Hakanson, 1980), which is a commonly method for heavy metals risk assessment (Gao et al., 2014). The calculation of RI is as follows:

$$E_r^i = T_r^i \times P_i, \tag{4}$$

$$RI = \sum_{i=1}^{n} E_r^i = \sum_{i=1}^{n} T_r^i \times P_i = \sum_{i=1}^{n} T_r^i \times \frac{C_n}{B_n}, \quad (5)$$

where E_r^i is the potential ecological risk factor of heavy metal i; and T_r^i is the toxicity response factor of heavy metal i (the T_r^i for Cu, Zn, Pb, As, Cd, and Cr is 5, 1, 5, 10, 30, and 2, respectively). According to the calculation results of RI, we also classified the pollution degree of heavy metals, as shown in Table 1.

Table 1 Classification of potential ecological risk

E_r^i	Potential ecological risk level	RI	Potential ecological risk level
<40	Low ecological risk	<150	Low ecological risk
40–80	Moderate ecological risk	150–300	Moderate ecological risk
80–160	Considerable ecological risk	300–600	Considerable ecological risk
160–320	Very high ecological risk	>600	Very high ecological risk
>320	Serious ecological risk		

Note: E_r^i, potential ecological risk factor of a single heavy metal; RI, potential ecological risk index.

2.3.4 Human health risk assessment

In this study, we consulted the Exposure Factors Handbook (U.S. Environmental Protection Agency, 2011) to assess carcinogenic and noncarcinogenic risks of heavy metals (Young et al., 2022). There are three ways humans are exposed to heavy metals: oral ingestion, inhalation, and dermal absorption. The equations for the average daily exposure, noncarcinogenic risk, and carcinogenic risk are provided as follows:

$$ADD_{\text{ing}} = \frac{C_n \times IR_{\text{ing}} \times EF \times ED \times 10^{-6}}{BW \times AT}, \quad (6)$$

$$ADD_{\text{der}} = \frac{C_n \times SL \times SA \times ABS \times EF \times ED \times 10^{-6}}{BW \times AT}, \quad (7)$$

$$ADD_{\text{inh}} = \frac{C_n \times IR_{\text{inh}} \times ED \times EF}{BW \times PEF \times AT}, \quad (8)$$

where ADD_{ing} is the average daily intake of heavy metals by oral ingestion (mg/(kg·d)); IR_{ing} is the ingestion rate by oral ingestion (mg/d); EF is the frequency of exposure (d/a); ED is the exposure duration (a); BW is the body weight (kg); AT is the average exposure time (d); ADD_{der} is the average daily intake of heavy metals by dermal absorption (mg/(kg·d)); SL is the adherence factor (mg/(cm^2·d)); SA is the skin exposure area (cm^2); ABS is the skin exposure factor; ADD_{inh} is the average daily intake of heavy metals by inhalation (mg/(kg·d)); IR_{inh} is the ingestion rate by inhalation (m^3/d); and PEF is the peak expiratory flow (m^3/kg).

$$HI = \sum HQ = \sum \frac{ADD}{RfD}, \quad (9)$$

$$TCR = \sum CR = \sum ADD \times SF, \quad (10)$$

where HQ and CR are the noncarcinogenic and carcinogenic risks for a single heavy metal, respectively; HI and TCR are the noncarcinogenic and carcinogenic risks for multiple heavy metals, respectively; ADD is the daily average exposure dose for noncarcinogenic risks (mg/(kg·d)); RfD is the reference dose (mg/(kg·d)); and SF is the safety factor. According to the Exposure Factors Handbook (U.S. Environmental Protection Agency, 2011), we concluded that when $CR<10^{-6}$, heavy metals pose little or no hazard to humans; when $10^{-6}<CR<10^{-4}$, heavy metals are in the acceptable range to humans; and when $CR>10^{-4}$, heavy metals pose an unacceptable risk to humans.

2.4 Statistical methods

We used SPSS 22.0 software to conduct descriptive statistics of soil heavy metals content and soil

physical-chemical properties. Correlation analysis of the heavy metals content with soil physical-chemical properties was performed using SPSS 22.0 software. OriginPro software was used to analyze the heavy metals content and soil physical-chemical properties at different soil depths. The spatial distribution of heavy metals risk was mapped using ArcGIS 10.2 software and the ordinary kriging method. Correlation analysis, principal component analysis (PCA), and cluster analysis were used to identify the sources of heavy metals in soils.

3 Results

3.1 Descriptive statistics of soil heavy metals

The results of heavy metals content in the study area are shown in Figure 2. The average content of Zn, As, Pb, Cu, Cr, and Cd at 0–5 cm soil depth was 671, 425, 235, 163, 95, and 4 mg/kg, respectively, which were higher than the risk screening values for soil contamination of agricultural land required by soil environmental quality—risk control standard for soil contamination of agricultural land (Ministry of Ecology and Environment of the People's Republic of China, 2018). These results also exceeded the local (Chifeng City) soil heavy metals background value. The exceeding standard rate of As, Cd, Zn, Cu, Pb, and Cr was 78%, 73%, 58%, 53%, 34%, and 10%, respectively, compared with the risk screening values (Table S1). The mean content of Zn, As, Pb, Cu, Cr, and Cd at 5–10 cm soil depth was 660, 354, 200, 162, 88, and 3 mg/kg, respectively, which exceeded the background values by 18, 45, 11, 11, 2, and 64 times, respectively. The content of As, Cd, Zn, Cu, Pb, and Cr at 5–10 cm soil depth exceeded the risk screening values by 73%, 66%, 56%, 49%, 29%, and 6%, respectively. At 10–20 cm soil depth, the content of As, Cd, Zn, Cu, Pb, and Cr exceeded the background values by 17%, 32%, 9%, 10%, 2%, and 104%, respectively, and the risk screening values by 64%, 62%, 52%, 41%, 23%, and 5%, respectively. The maximum exceeding standard rate of As and Cd was most severe at different soil depths, and the exceeding standard rate decreased continuously with increasing soil depth. The pollution level of Cr was relatively light.

The coefficient of variation (CV) is an important indicator of data dispersion and is graded as weak variability (<10%), moderate variability (10%–100%), and strong variability (>100%). The CV of Cr content was 87% and showed a moderate variability (Table S1). The CV values of other heavy metals showed strong variability, with As showing the largest CV (220%).

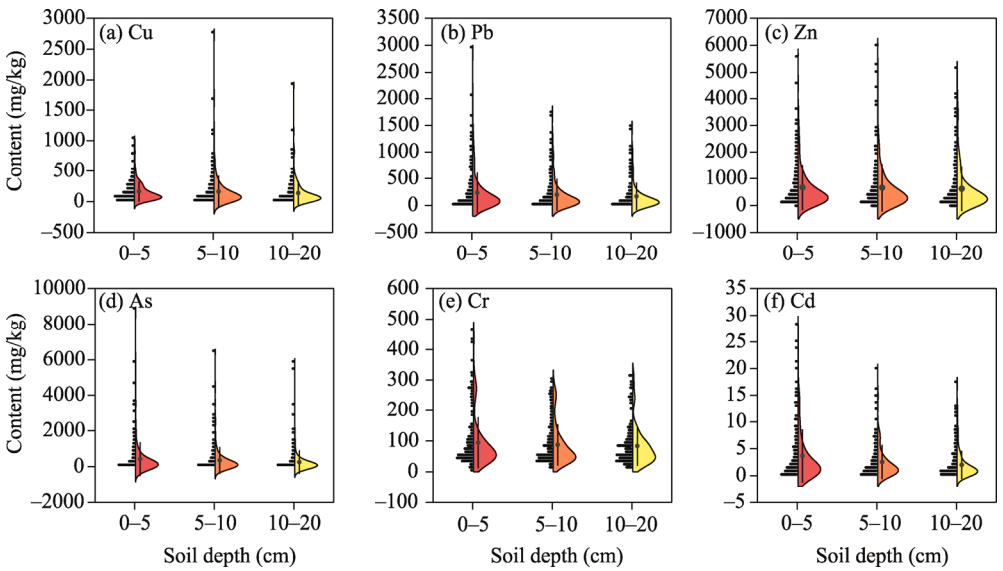

Fig. 2 Content of cuprum (Cu; a), lead (Pb; b), zinc (Zn; c), arsenic (As; d), chromium (Cr; e), cadmium (Cd; f), at different soil depths. The bar chart and the width of violin chart represent the frequency of the data. The black dots represent the medians. The bars represent the 95% confidence interval.

3.2 Soil physical-chemical properties

Soil pH and EC affect a variety of soil properties, which in turn affect the biological activity of soil heavy metals. Results of the statistical analysis of soil physical-chemical properties are shown in Figure 3. At 0–5 cm soil depth, the EC ranged from 57 to 3098 mS/cm, with a mean value of 415 mS/cm; the mean value of soil pH was 7.7, and 16 soil samples had a pH value lower than 6.5. At 5–10 cm soil depth, the EC ranged from 37 to 2841 mS/cm, with a mean value of 455 mS/cm; the value of soil pH varied from 2.4 to 8.5, with a mean value of 7.7. At 10–20 cm soil depth, the mean value of EC and pH was 557 mS/cm and 7.6, respectively. Most of the soil samples in the study area were weakly alkaline, and with the deepening of the soil depth, pH gradually decreased and EC gradually increased.

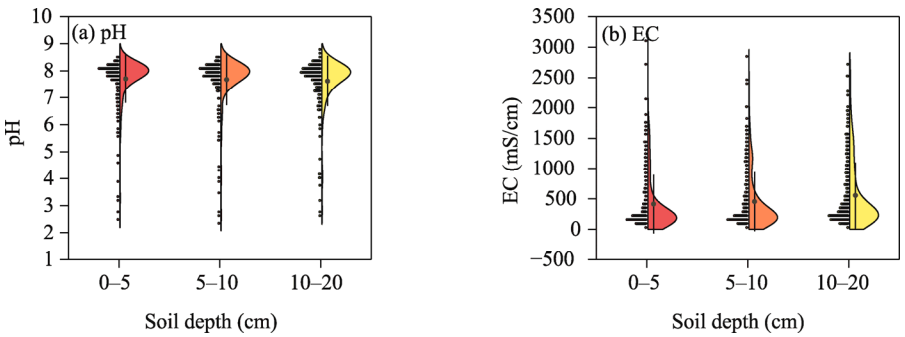

Fig. 3 Soil pH (a) and electrical conductivity (EC; b) at different soil depths. The bar chart and the width of violin chart represent the frequency of the data. The black dots represent the medians. The bars represent the 95% confidence interval.

3.3 Spatial distribution of the content of heavy metals in soils

The spatial distribution of the content of heavy metals in soils of the study area was obtained by the ordinary kriging method (Fig. 4). The distributions of the six heavy metals (Cu, As, Pb, Zn, Cr, and Cd) were very similar, showing a downward trend from southwest to northeast. High Cr contents were concentrated in the west of the tailings pond, while high As contents were concentrated in the southeast of the tailings pond. The highest content of heavy metals occurred at 0–5 cm soil depth and the lowest content of heavy metals occurred at 10–20 cm soil depth (Figs. S1 and S2).

3.4 Spatial distribution of heavy metals pollution in soils

3.4.1 Spatial distribution of I_{geo}

A map of the spatial distribution of soil heavy metals pollution was drawn using the ordinary kriging method (Fig. 5). Results showed that the pollution level near the tailing ponds is more severe. The spatial distribution characteristics of different heavy metals greatly varied. The pollution degree of heavy metals tended to decrease with increasing soil depth. The 0–5 cm soil layer was the most polluted. The highest As pollution index was found at 0–10 cm soil depth in the southern and eastern parts of the tailings pond, with severe pollution (I_{geo}>5). Cd pollution was more serious in the southwest of the tailings pond, with I_{geo} ranging from 2 to 5.

In the study area, 7% of the soil was severely polluted by As, and 10% of the soil was moderately polluted by As. Additionally, 2% of the soil was heavily polluted by Cd, while 6% of the soil was lightly polluted by Cd (Fig. S3). The pollution degree of Cu, Pb, and Zn around the tailings pond was light. The soil in the western and southern parts of the tailings pond was moderately polluted by Cu (2<I_{geo}<3). In the northwest and southeast of the tailings pond, soil was moderately polluted by Zn (2<I_{geo}<3). Soil contaminated by Zn, Cu, and Pb accounted for 9%, 3%, and 5% of the moderately polluted areas, respectively, and 2%, 1%, and 1% of the heavily polluted areas, respectively.

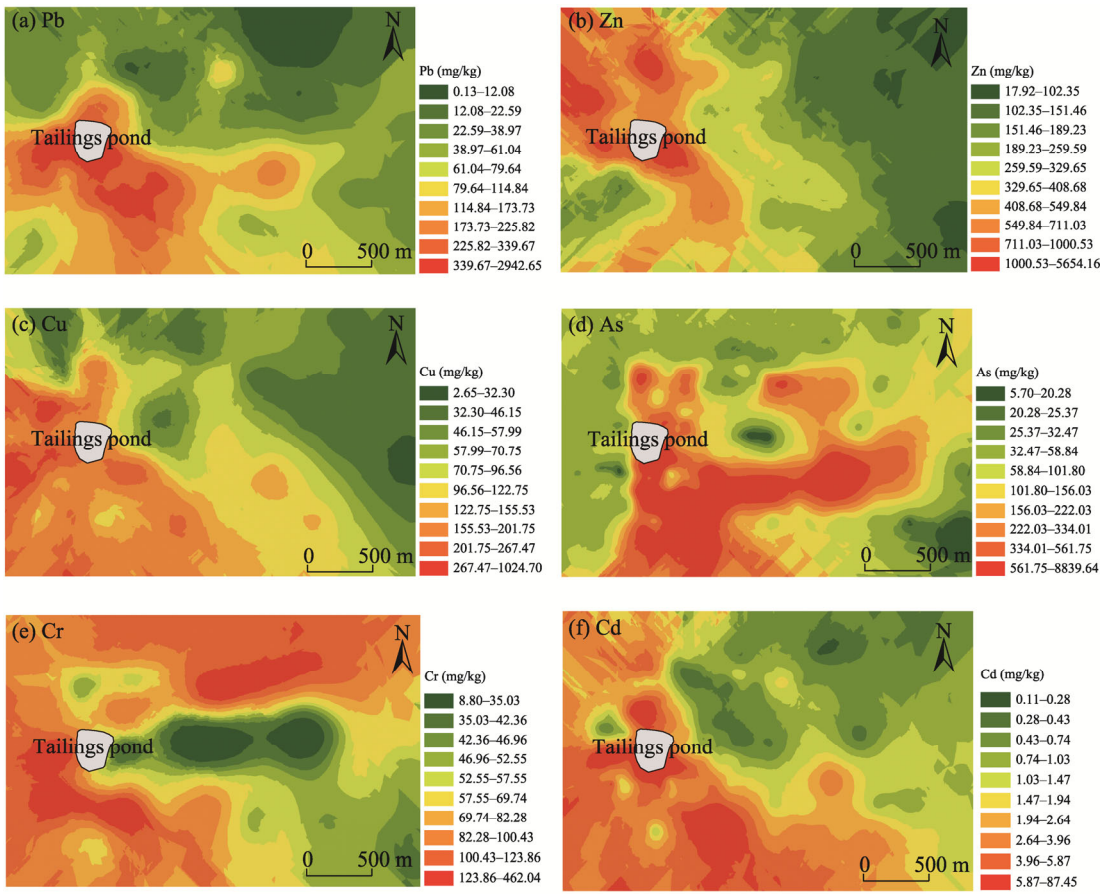

Fig. 4 Spatial distribution of the content of Pb (a), Zn (b), Cu (c), As (d), Cr (e), and Cd (f) at 0–5 cm soil depth

3.4.2 Overall pollution levels of heavy metals based on the Nemerow general pollution index (P_N)

As, Cd, Pb, Cu, and Zn reached severe pollution levels in the study area. The pollution level of As was the most severe, with P_N ranging from 127 to 250 (Fig. 6). The pollution level of Cd was also more severe, with P_N greater than or equal to 41. The pollution level of Cr was light, with a P_N value of 1 at 0–5 cm soil depth. P_N was less than 1 at 5–20 cm soil depth, indicating a state of no pollution. In summary, the pollution level of As and Cd in the study area was severe, and the pollution level of Cr was light.

3.4.3 Comprehensive pollution status of heavy metals based on the potential ecological risk index (*RI*)

We used the soil environmental quality—risk control standard for soil contamination of agricultural land (Ministry of Ecology and Environment of the People's Republic of China, 2018) as the baseline value to evaluate soil pollution in the study area. The ordinary kriging method was used to draw the spatial distribution of *RI* at different soil depths in the study area (Fig. 7).

The values of potential ecological risk factor of a single heavy metal (E_r^i) of Cr, Zn, Cu, and Pb at different soil depths in the study area were lower than 40, which indicated that these heavy metals are at a low ecological risk level (Table S2). The E_r^i value of As ranged from 95 to 160, indicating a considerable ecological risk. The E_r^i value of Cd ranged from 123 to 209, showing a very high ecological risk. The percentage of Cd causing serious ecological risk to soil was greater than that of As (Fig. S4). Therefore, the ecological risk of Cd pollution was higher than that of As pollution. The *RI* was 388, 273, and 291 at 0–5, 5–10, and 10–20 cm soil depths, respectively. The 0–5 cm soil layer was at a considerable ecological risk, and the 5–20 cm soil layer was at a moderate ecological risk (Table S2).

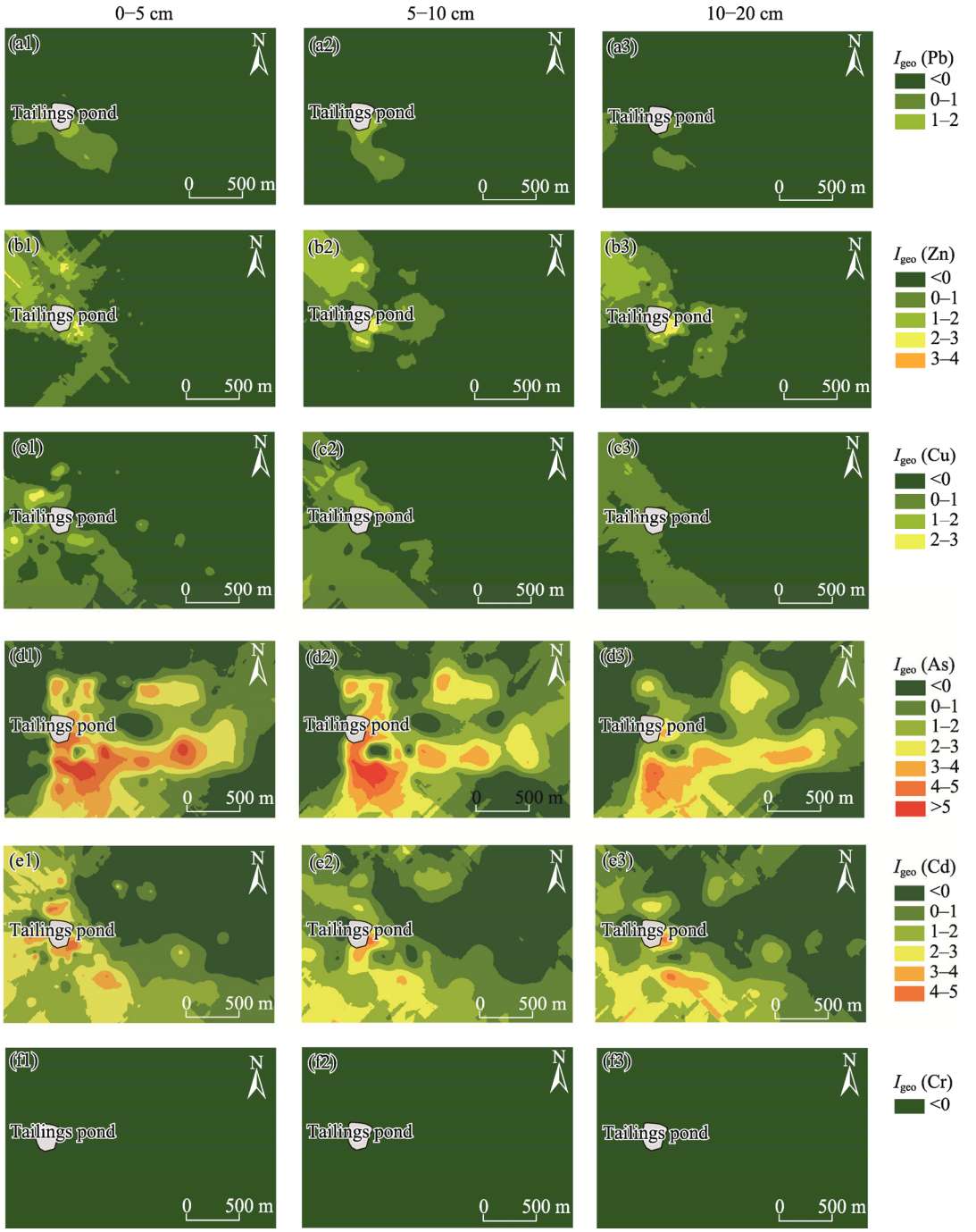

Fig. 5 Spatial distribution of heavy metals pollution level at 0–5, 5–10, and 10–20 cm soil depths based on the Geo-accumulation index (I_{geo}). (a1–a3), Pb; (b1–b3), Zn; (c1–c3), Cu; (d1–d3), As; (e1–e3), Cd; (f1–f3), Cr.

As showing in Figure 7, the heavy metals pollution at 0–5 cm soil depth was more severe in the southern area of the tailings pond. There was a very high ecological risk in a small part of the western and northern areas of the tailings pond. The areas with very high ecological risk and considerable ecological risk accounted for 20% and 13% of the total area, respectively. The pollution degree at 5–20 cm soil depth gradually decreased, and the heavily polluted areas were mainly concentrated in the southern part of the study area. The area with very high ecological risk at 5–10 cm soil depth was 11%, which was 8% lower than the ecological risk of topsoil (0–5 cm).

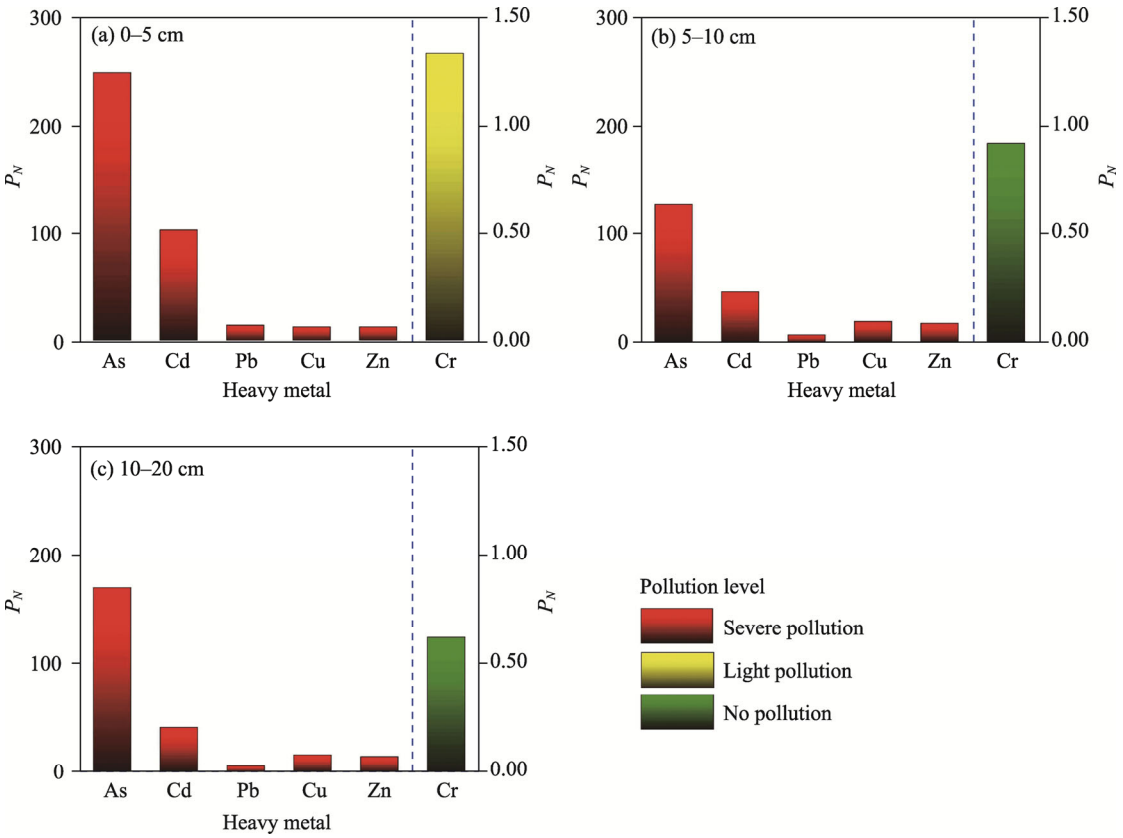

Fig. 6 Nemerow general pollution index (P_N) of heavy metals at 0–5 (a), 5–10 (b), and 10–20 (c) cm soil depths

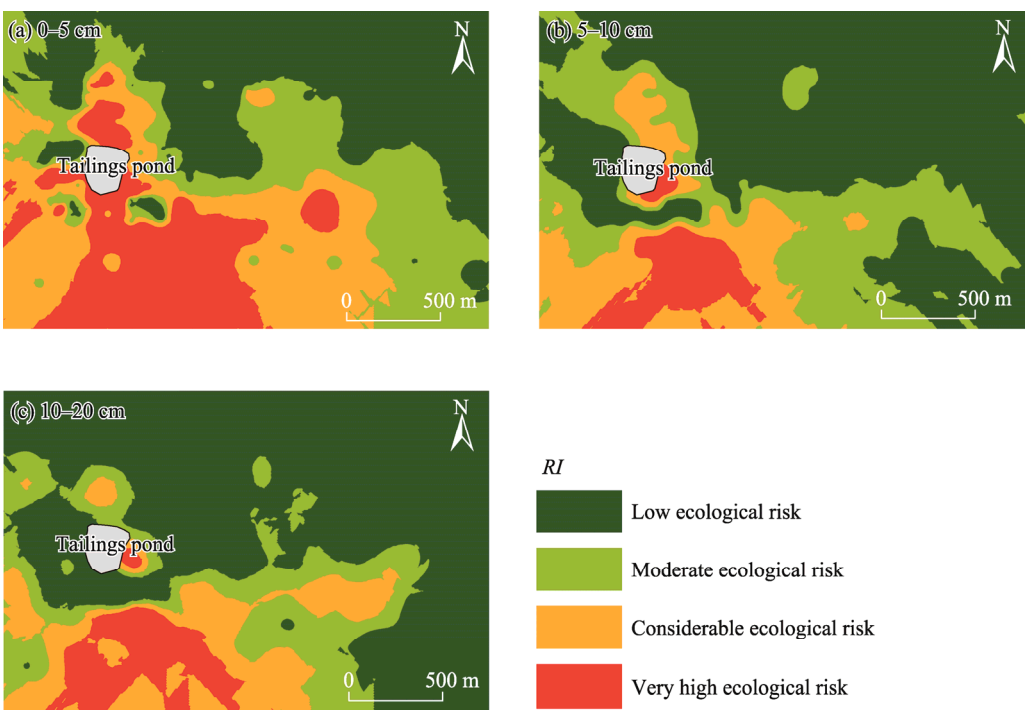

Fig. 7 Pollution distribution map based on potential ecological risk index (*RI*) at 0–5 (a), 5–10 (b), and 10–20 (c) cm soil depths

The area with considerable ecological risk at 5–10 cm soil depth was 13%, showing no significant variation compared to the topsoil (0–5 cm). The areas with very high ecological risk and considerable ecological risk at 10–20 cm soil depth dropped to 7% and 10% of the total area, respectively (Fig. S5). The results of the *RI* showed that the pollution level of the topsoil (0–5 cm) was the most serious, and the *RI* showed a decreasing trend with the deepening of the soil layer.

3.4.4 Health risk assessment

The noncarcinogenic health risks of five heavy metals, including Cu, Zn, As, Pb, and Cd, were assessed in this study. The results showed that As, Zn, and Pb pose high noncarcinogenic risks to human health (Table 2). The ranking of heavy metals intake levels through different pathways was as follows: HQ_{ing}>HQ_{der}>HQ_{inh} (where HQ_{ing} HQ_{der}, and HQ_{inh} are noncarcinogenic risk of a single heavy metal through oral ingestion, dermal absorption, and inhalation, respectively). The noncarcinogenic risks for multiple heavy metals (*HI*) for children was 1.2, indicating that heavy metals in the study area pose a potential noncarcinogenic health risk threat to children. All other exposure pathways had an *HI* value of less than 1.0, indicating no significant risk to human health.

Table 2 Assessment of reference dose (*RfD*) values and noncarcinogenic health risks of different exposure pathways of soil heavy metals in different populations

Heavy metal	RfD_{ing} mg/(kg·d)	RfD_{der} mg/(kg·d)	RfD_{inh} mg/(kg·d)	HQ_{ing}		HQ_{der}		HQ_{inh}	
				Child	Adult	Child	Adult	Child	Adult
Cu	4.0×10^{-2}	1.2×10^{-2}	-	1.6×10^{-4}	9.2×10^{-5}	$3{,}8\times10^{-7}$	3.2×10^{-7}	3.8×10^{-9}	8.6×10^{-9}
Zn	3.0×10^{-1}	6.0×10^{-2}	-	6.4×10^{-4}	3.8×10^{-4}	1.6×10^{-6}	1.3×10^{-6}	1.5×10^{-8}	3.5×10^{-8}
As	3.0×10^{-4}	1.2×10^{-4}	3.5×10^{-6}	3.4×10^{-4}	2.0×10^{-4}	8.3×10^{-7}	7.0×10^{-7}	8.2×10^{-9}	1.8×10^{-8}
Pb	3.5×10^{-3}	5.3×10^{-4}	8.2×10^{-5}	1.8×10^{-4}	1.0×10^{-4}	4.3×10^{-7}	3.6×10^{-7}	4.3×10^{-9}	9.6×10^{-9}
Cd	1.0×10^{-3}	1.0×10^{-5}	2.4×10^{-6}	2.3×10^{-6}	1.4×10^{-6}	5.7×10^{-9}	4.8×10^{-9}	5.6×10^{-11}	1.3×10^{-10}
HI	-	-	-	1.2	7.0×10^{-1}	8.2×10^{-3}	6.9×10^{-3}	2.4×10^{-3}	5.4×10^{-3}

Note: RfD_{ing}, reference dose of a single heavy metal through oral ingestion; RfD_{der}, reference dose of a single heavy metal through dermal absorption; RfD_{inh}, reference dose of a single heavy metal through inhalation; HQ_{ing}, noncarcinogenic risk of a single heavy metal through oral ingestion; HQ_{der}, noncarcinogenic risk of a single heavy metal through dermal absorption; HQ_{inh}, noncarcinogenic risk of a single heavy metal through inhalation; *HI*, noncarcinogenic risks for multiple heavy metals. -, no value.

The carcinogenic health risk of heavy metals was ranked as CR_{ing}>CR_{der}>CR_{inh} (where CR_{ing} CR_{der}, and CR_{inh} are carcinogenic risk of a single heavy metal through oral ingestion, dermal absorption, and inhalation, respectively). As and Pb posed a carcinogenic risk to human health, while the carcinogenic risk of Ca was within an acceptable range. Dermal absorption and inhalation to heavy metals did not pose a carcinogenic risk to human health (Table 3). According to the Exposure Factors Handbook (U.S. Environmental Protection Agency, 2011) for children and adults, we found that oral exposure to heavy metals has an unacceptable carcinogenic risk, dermal exposure to heavy metals has an acceptable risk, and inhalation of heavy metals has no carcinogenic risk.

Table 3 Assessment of carcinogenic health risks of different exposure pathways of soil heavy metals in different populations

Heavy metal	CR_{ing}		CR_{der}		CR_{inh}	
	Child	Adult	Child	Adult	Child	Adult
As	3.4×10^{-4}	2.0×10^{-4}	8.3×10^{-7}	7.0×10^{-7}	8.2×10^{-9}	1.8×10^{-8}
Pb	1.8×10^{-4}	1.0×10^{-4}	4.3×10^{-7}	3.6×10^{-7}	4.3×10^{-9}	9.6×10^{-9}
Cd	2.3×10^{-6}	1.4×10^{-6}	5.7×10^{-9}	4.8×10^{-9}	5.6×10^{-11}	1.3×10^{-10}

Note: CR_{ing}, carcinogenic risk of a single heavy metal through oral ingestion; CR_{der}, carcinogenic risk of a single heavy metal through dermal absorption; CR_{inh}, carcinogenic risk of a single heavy metal through inhalation.

3.5 Multivariate statistical analysis results

3.5.1 Correlation analysis among heavy metals

Correlation analysis is an important basis for determining the source of heavy metals. The normality test was performed by SPSS software, and all the six heavy metals were non-normal distribution with outliers. Therefore, the Spearman correlation analysis was used in this study (Table 4). Cd showed highly significant positive correlations with Pb (r=0.84), Cu (r=0.58), and As (r=0.49); Cu showed significant positive correlations with Zn (r=0.35) and Pb (r=0.53); Pb showed positive correlations with As (r=0.49) and Zn (r=0.33); and Cd showed a positive correlation with Zn (r=0.41). There were positive correlations among Cu, Zn, Pb, Cd, and As, suggesting that they may have similar origins. Cr was significantly positively correlated with Pb, while Cr was significantly negatively correlated with Zn. The positive correlation between Cr and other heavy metals was not significant, indicating that the sources of Cr and other heavy metals are different. In addition, the pH was negatively correlated with Cu, Pb, Zn, As, and Cd and positively correlated with Cr. Among them, pH, EC, and Cu were significantly correlated with Zn; therefore, soil pH and EC in the study area may have a greater influence on the enrichment of Cu and Zn in soils.

Table 4 Spearman correlation analysis of heavy metals and soil physical-chemical parameters

	Cu	Zn	Cr	As	Cd	Pb	EC	pH
Cu	1.000							
Zn	0.351**	1.000						
Cr	0.103	–0.355**	1.000					
As	0.196**	0.199**	–0.097	1.000				
Cd	0.583**	0.411**	0.116	0.485**	1.000			
Pb	0.532**	0.331**	0.214**	0.491**	0.840**	1.000		
EC	0.382**	0.366**	–0.134*	0.138*	0.282**	0.229**	1.000	
pH	–0.202**	–0.370**	0.226**	–0.045	–0.115	–0.059	–0.476**	1.000

Note: EC, electrical conductivity; *, P<0.05 level; **, P<0.01 level.

3.5.2 Principal component analysis (PCA)

Furthermore, in order to investigate the interrelationships among heavy metals and the possible sources of heavy metals, we conducted a PCA using SPSS software. The results of PCA are presented in Table 5.

Table 5 Principal component analysis (PCA) of heavy metals in soils of the study area

PC	Initial eigenvalue			Sum of squared loadings		
	Eigenvalue	Explain variance (%)	Cumulative variance (%)	Eigenvalue	Explain variance (%)	Cumulative variance (%)
1	2.583	43.054	43.054	2.583	43.054	43.054
2	1.436	23.937	66.991	1.436	23.937	66.991
3	0.814	13.566	80.557	0.814	13.566	80.557
4	0.575	9.580	90.137			
5	0.327	5.449	95.586			
6	0.265	4.414	100.000			

Note: PC, principal component.

From the results of PCA (Table 5), we can see that the first three principal components of the six heavy metals explained 80.557% of the total variance, so the analysis of the first three principal components provides most information about the contents of Cu, Zn, As, Pb, Cd, and Cr

(Fig. 7). The PC1 (PC is principal component) explained 43.054% of the total variance, mainly contributed by Pb, Cd, and Zn, with rotation factor loadings of 0.87, 0.86 and 0.64, respectively. The PC2 explained 23.937% of the total variance, mainly contributed by Cr and As, with rotation factor loadings of 0.81 and 0.51, respectively. The PC3 explained 13.566% of the total variance, mainly contributed by Cu, with a rotation factor loading of 0.84. The results indicated that there are three main sources of soil heavy metals in the study area.

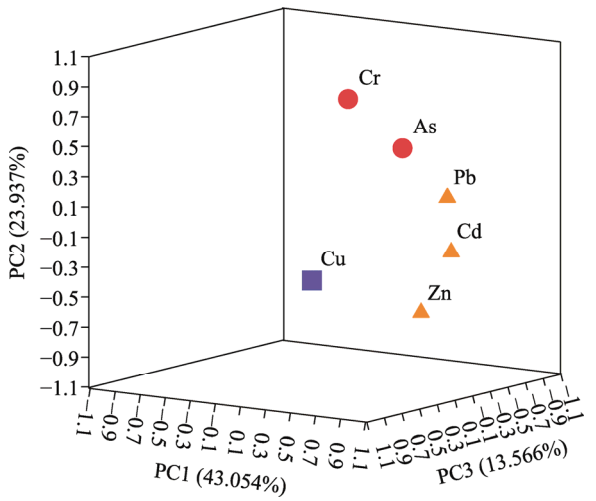

Fig. 8 Principal component analysis (PCA) of heavy metals in soils of the study area. PC, principal component.

3.5.3 Cluster analysis

Hierarchical clustering dendrogram can directly reflect the correlation among heavy metals and reveal the sources of soil heavy metals. Results of the cluster analysis (the Ward method was chosen for the cluster analysis, and the Euclidean distance method was chosen for the measurement of interval) were used to group the six heavy metals into three categories (Fig. 8). The first group included Cd, Pb, and Zn, the second group included Cr and As, and the third group included Cu.

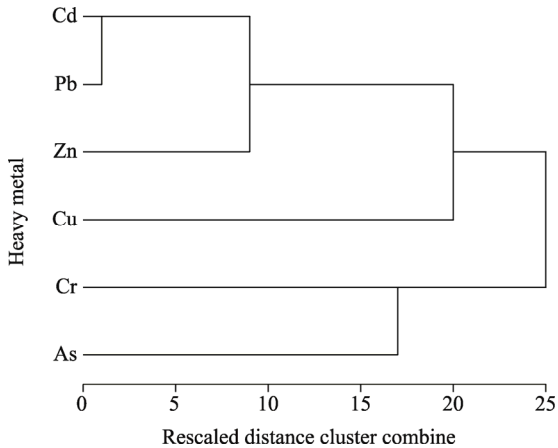

Fig. 9 Cluster analysis of heavy metals in soils of the study area

4 Discussion

4.1 Effects of heavy metals pollution risk

Heavy metals are found in soil during natural formation and are generally harmless to the

environment due to their low content (Muhammad et al., 2022). However, with the increase of the frequency of human activities, the content of heavy metals in the soil continues to increase, resulting in the content of heavy metals in the affected soil being much higher than the natural background value. Therefore, heavy metals pose a serious risk to ecosystems and human health (Li et al., 2018).

In this study, areas with a higher degree of soil heavy metals pollution and ecological risk are concentrated in the northwest and southeast of the tailings pond. Therefore, heavy metals generally migrate from northwest to southeast. The study area features a rugged topography with significant variations in elevation, gradually decreasing from northwest to southeast. The distribution of heavy metals is more consistent with wind direction and topography, which indicates that wind direction and topography have an influence on heavy metals migration. This promotes heavy metals particulate matter entering the surrounding soil through the air. However, the heavy metals content decreases with increasing soil depth (Figs. 4, S1, and S2). Heavy metals such as Cd, As, and Zn mainly accumulate on the surface, indicating that the soils may be heavily polluted by exogenous sources such as atmospheric deposition and industrial and agricultural activities (Song et al., 2018). The heavy metals content in soils far away from the tailings pond is significantly lower than that around the tailings pond, and the vertical change of the heavy metals content is small (Zhao et al., 2021).

Results of the correlation analysis between soil pH and heavy metals provide another concern. Soil pH can regulate activities related to the toxicity and transformation of heavy metals in soils (Xu et al., 2017). In this study, pH is negatively correlated with all heavy metals except Cr, which indicates that the lower the pH, the higher the heavy metals content. The effectiveness of heavy metals in soil solution increases with the decrease of pH (Inka et al., 2016). Therefore, the increased toxicity of heavy metals caused by soil acidification requires special attention.

4.2 Analysis of the sources of heavy metals

Human activities have an impact on the content of Cu, Zn, Cd, Pb, Cr, and As in soils. A combination of multivariate statistical analysis and spatial analysis was used to analyze the sources of heavy metals.

Both correlation analysis and PCA suggest that Cd, Pb, and Zn may have a common source. Notably, the main source of Pb and Zn is the accumulation of wastewater and sludge in the tailings pond (Ma et al., 2015). Results of the spatial distribution of heavy metals in this study show that Pb and Zn are mainly concentrated near the tailings pond with characteristics of diffusion to surrounding soils. This result indicates that Pb and Zn are more influenced by the tailings pond. The regions with high Zn content are mainly located in the northwest of the tailings pond. The mining area processes and refines the crude ore into concentrate. This process generates large quantities of toxic and hazardous substances containing Zn, and the release of aerosols and dust can contaminate nearby soils (Liu et al., 2018). It is inferred that the main source of Cd is the accumulation of wastewater and slag. Cd is extremely harmful to humans and has a very low threshold compared to other heavy metals. Under the same conditions, Cd has higher migration capacity than Pb and Zn, and is more likely to contaminate deep soils and groundwater. As a result, the pollution level of Cd in soils of the study area is higher.

The PC2 includes Cr and As, with most of the Cr accumulation in the study area close to the soil background value. Only a few soils close to the tailings pond were lightly contaminated by Cr. The main source of Cr in soils is the soil parent material (Liang et al., 2017; Liu et al., 2021). In addition, the soil in the study area generally exhibits high levels of As content. Studies have shown that Inner Mongolia is the region with the highest As emission potential in China (Wei et al., 2020). With the passage of time, the background value of As in the study area gradually increases. Combined with the correlation analysis, it is clear that Cr and As are homologous. Therefore, the main source of Cr is the soil parent material, and the study area has a high background value of As.

The PC3 includes Cu. As shown in Figure 4, the areas with high Cu content are concentrated in

the northwest of the tailings pond. The investigation found a Cu mine approximately 1 km northwest of the tailings pond. The mining and smelting of Cu produces large amounts of elemental Cu, which can accumulate in surrounding soils through atmospheric deposition (Nezat et al., 2017). The dominant wind direction in the study area is northwester; therefore, the main source of Cu is likely the Cu mines in the northwestern part of the study area.

Additionally, most chemical fertilizers and pesticides contain a certain amount of heavy metals. Even if chemical fertilizers and pesticides meet national standards, agricultural soil will be continuously enriched with heavy metals in the process of long-term application (Fei et al., 2019).

5 Conclusions

In this study, we investigated the heavy metals pollution in soils around a typical Pb and Zn mining area in eastern Inner Mongolia. The content and distribution of Zn, As, Pb, Cu, Cr, and Cd were analyzed. The ecological risk of heavy metals was assessed, and a traceability study was conducted. The most severely polluted heavy metals were found at 0–5 cm soil depth. The average content of Zn, As, Pb, Cu, Cr, and Cd was 670, 424, 235, 162, 94 and 4 mg/kg, respectively. There were significant differences in heavy metals contents in different regions, which were mainly influenced by topography and wind direction. Pollution assessment showed that the ecological risk of heavy metals near the tailings pond is the highest, and the impact range is the largest with some areas reaching severe pollution levels. The human health risk assessment showed that the three pathways of exposure for carcinogenic and noncarcinogenic risks are ranked as inhalation>oral ingestion>dermal absorption. The noncarcinogenic risks for As, Pb, and Zn were high, and in terms of total noncarcinogenic risk, oral ingestion posed a potential threat to children, whereas the other pathways did not pose a significant threat to humans. The overall carcinogenic risk was high for oral ingestion, within acceptable limits for dermal absorption, and did not pose a carcinogenic risk for inhalation. Analysis of the sources of heavy metals showed that the tailings pond contributed to the pollution of Pb, Zn, and Cd. The source of Cr was the soil parent material, while As was mainly due to high background values in the study area; and the source of Cu was mainly from nearby Cu mining and smelting activities. The remediation strategies in this region should focus on controlling the emissions of heavy metal at source. Combined with different remediation strategies, economical, rapid, and efficient soil remediation actions should be taken.

Conflict of interest

The authors declare that they have no known competing financial interests or personal relationships that could have appeared to influence the work reported in this paper.

Acknowledgements

This research was supported by the Inner Mongolia Autonomous Region Major Science and Technology Special Project (2019ZD001). We would like to express our gratitude to the anonymous reviewers for their valuable comments.

Author contributions

Conceptualization: XIE Shicheng; Data curation: XIE Shicheng; Methodology: LAN Tian, XING An; Investigation: XIE Shicheng, CHEN Chen, MENG Chang, WANG Shuiping, XU Mingming; Formal analysis: XIE Shicheng; Writing - original draft preparation: XIE Shicheng; Writing - review and editing: XIE Shicheng, LAN Tian; Funding acquisition: HONG Mei; Resources: HONG Mei; Supervision: HONG Mei; Project administration: HONG Mei; Software: XIE Shicheng; Validation: XIE Shicheng; Visualization: XIE Shicheng.

References

Cheng X F, Danek T, Drozdova J, et al. 2018. Soil heavy metal pollution and risk assessment associated with the Zn–Pb mining

region in Yunnan, Southwest China. Environmental Monitoring and Assessment, 190: 194, doi: 10.1007/s10661-018-6574-x.

Chun F, Na R, Zhang W, et al. 2021. Spatial heterogeneity of soil heavy metal content in Baiyinhua mining area, Inner Mongolia, China. The Journal of Applied Ecology, 32(2): 601–608.

Din I U, Muhammad S, Rehman I U. 2022. Heavy metal(loid)s contaminations in soils of Pakistan: A review for the evaluation of human and ecological risks assessment and spatial distribution. Environmental Geochemistry and Health, 45(5): 1991–2012.

Dong B, Zhang R Z, Gan Y D, et al. 2019. Multiple methods for the identification of heavy metal sources in cropland soils from a resource-based region. Science of the Total Environment, 651(2): 3127–3138.

Du B Y, Zhou J, Lu B X, et al. 2020. Environmental and human health risks from cadmium exposure near an active lead-zinc mine and a copper smelter, China. Science of the Total Environment, 720, doi: 10.1016/j.scitotenv.2020.137585.

Fei X F, Xiao R, Christakos G, et al. 2019. Comprehensive assessment and source apportionment of heavy metals in Shanghai agricultural soils with different fertility levels. Ecological Indicators, 106, doi: 10.1016/j.ecolind.2019.105508.

Gao C Y, Lin Q X, Bao K S, et al. 2014. Historical variation and recent ecological risk of heavy metals in wetland sediments along Wusuli River, Northeast China. Environmental Earth Sciences, 72(11): 4345–4355.

Gao Y F, Liu H L, Liu G X. 2017. The spatial distribution and accumulation characteristics of heavy metals in steppe soils around three mining areas in Xilinhot in Inner Mongolia, China. Environmental Science and Pollution Research, 24(32): 25416–25430.

Hakanson L. 1980. An ecological risk index for aquatic pollution control. A sedimentological approach. Water Research, 14(8): 975–1001.

Hu Z G, Wang C S, Li K Q, et al. 2018. Distribution characteristics and pollution assessment of soil heavy metals over a typical nonferrous metal mine area in Chifeng, Inner Mongolia, China. Environmental Earth Sciences, 77(18): 1, doi: 10.1007/s12665-018-7771-1.

Inka R, Helinä H. 2016. Oxidation mechanisms and chemical bioavailability of chromium in agricultural soil-pH as the master variable. Applied Geochemistry, 74: 84–93.

Li L M, Wu J, Lu J, et al. 2018. Distribution, pollution, bioaccumulation, and ecological risks of trace elements in soils of the northeastern Qinghai-Tibet Plateau. Ecotoxicology and Environmental Safety, 166(1): 345–353.

Li X L, Yang J X, Fan Y F, et al. 2021. Rapid monitoring of heavy metal pollution in lake water using nitrogen and phosphorus nutrients and physicochemical indicators by support vector machine. Chemosphere, 280: 130599, doi: 10.1016/j.chemosphere.2021.130599.

Li Y J, Li P J, Yang G F, et al. 2003. Diagnosis of heavy metal contaminated soil toxicity by the daphnia magna method. Journal of Agricultural Environmental Science, 22(2): 159–162. (in Chinese)

Liang J, Feng C T, Zeng G M, et al. 2017. Spatial distribution and source identification of heavy metals in surface soils in a typical coal mine city, Lianyuan, China. Environmental Pollution, 225(17): 681–690.

Liu F, Yang Z, Yang R H, et al. 2022. Migration characteristics and potential ecological environment evaluation of metal elements in surface soil. KSCE Journal of Civil Engineering, 26(5): 2068–2076.

Liu H W, Zhang Y, Yang J S, et al. 2021. Quantitative source apportionment, risk assessment and distribution of heavy metals in agricultural soils from southern Shandong Peninsula of China. Science of The Total Environment, 767: 144879, doi: 10.1016/j.scitotenv.2020.144879.

Liu R P, Xu Y N, Zhang J H, et al. 2020. Effects of heavy metal pollution on farmland soils and crops: A case study of the Xiaoqinling Gold Belt, China. China Geology, 3(3): 402–410.

Liu S Y, Tian S H, Li K X, et al. 2018. Heavy metal bioaccessibility and health risks in the contaminated soil of an abandoned, small-scale lead and zinc mine. Environmental Science & Pollution Research, 25(15): 15044–15056.

Liu Y X, Wu L B, Dong H J. 2019. Analysis of heavy metal pollution in urban surface soil based on the optimized N. L. Nemerow model. International Journal of Economics, Business and Management Research, 3(6): 126–141.

Loska K, Wiechuła D, Korus I. 2004. Metal contamination of farming soils affected by industry. Environment International, 30(2): 159–165.

Ma L, Sun J, Yang Z G, et al. 2015. Heavy metal contamination of agricultural soils affected by mining activities around the Ganxi River in Chenzhou, Southern China. Environmental Monitoring and Assessment, 187(12): 1–23.

Ministry of Ecology and Environment of the People's Republic of China, 2018. Soil environmental quality—risk control standard for soil contamination of agricultural land (GB 15618-2018). [2023-01-10]. http://s.dic.cool/S/6M2ZGrGf.

Muhammad H S, Shafaqat A, Muzammal R, et al. 2020. Influence of phosphorus on copper phytoextraction via modulating cellular organelles in two jute (*Corchorus capsularis* L.) varieties grown in a copper mining soil of Hubei Province, China. Chemosphere, 248: 126032, doi: 10.1016/j.chemosphere.2020.126032.

Muhammad S, Usman Q A. 2021. Heavy metal contamination in water of Indus River and its tributaries, Northern Pakistan: Evaluation for potential risk and source apportionment. Toxin Reviews, doi: 10.1080/15569543.2021.1882499.

Muhammad S. 2022. Evaluation of heavy metals in water and sediments, pollution, and risk indices of Naltar Lakes, Pakistan. Environmental Science and Pollution Research, 30(10): 28217–28226.

Müller G. 1969. Index of geoaccumulation in sediments of the Rhine River. GeoJournal, 2: 108–118.

Nezat C A, Hatch S A, Uecker T. 2017. Heavy metal content in urban residential and park soils: A case study in Spokane, Washington, USA. Applied Geochemistry, 78(1): 186–193.

Sehrish A, Muhammad S, Fatima H. 2021. Evaluation and risks assessment of potentially toxic elements in water and sediment of the Dor River and its tributaries, Northern Pakistan. Environmental Technology & Innovation, 21: 101333, doi: 10.1016/j.eti.2020.101333.

Shi T R, Zhang Y Y, Gong Y W, et al. 2019. Status of cadmium accumulation in agricultural soils across China (1975–2016): From temporal and spatial variations to risk assessment. Chemosphere, 230: 136–143.

Song S, Li Y J, Li L, et al. 2018. Arsenic and heavy metal accumulation and risk assessment in soils around mining areas: The Urad Houqi area in arid Northwest China as an example. International Journal of Environmental Research and Public Health, 15(11): 2410, doi: 10.3390/ijerph15112410.

Sun L, Guo D K, Liu K, et al. 2019. Levels, sources, and spatial distribution of heavy metals in soils from a typical coal industrial city of Tangshan, China. CATENA, 175: 101–109.

Sun Y Y, Zhao Z G, Liu X, et al. 2017. Environmental risk assessment of heavy metal contaminated soil in a concentrated nonferrous metal mining area in western Inner Mongolia. Journal of Inner Mongolia Normal University, 46(6): 853–860. (in Chinese)

U.S. Environmental Protection Agency. 2011. Exposure Factors Handbook. [2023-01-10]. http://refhub.elsevier.com/S0045-6535(23)01415-7/sref90.

Wang C, Yang Z F, Zhong C, et al. 2016. Temporal–spatial variation and source apportionment of soil heavy metals in the representative river–alluviation depositional system. Environmental Pollution, 216(16): 18–26.

Wang D L, Wang L, Liu J S, et al. 2018. Grassland ecology in China: Perspectives and challenges. Frontiers of Agricultural Science and Engineering, 5(1): 24–43.

Wei X D, Zhou Y T, Jiang Y J, et al. 2020. Health risks of metal(loid)s in maize (*Zea mays* L.) in an artisanal zinc smelting zone and source fingerprinting by lead isotope. Science of The Total Environment, 742: 140321, doi: 10.1016/j.scitotenv.2020.140321.

Xu L, Cui H B, Zheng X B, et al. 2017. Changes in the heavy metal distributions in whole soil and aggregates affected by the application of alkaline materials and phytoremediation. RSC Advances, 7(65): 41033–41042.

Young B, Ingwersen W W, Bergmann M, et al. 2022. A system for standardizing and combining U.S. environmental protection agency emissions and waste inventory data. Applied Sciences, 12(7): 1–16.

Yang F, Xie S Y, Hao Z H, et al. 2022. Geochemical quantitative assessment of mineral resource potential in the Da Hinggan Mountains in Inner Mongolia, China. Minerals, 12(4): 434, doi: 10.3390/min12040434.

Zhao X Q, Huang J, Zhu X Y, et al. 2021. Ecological effects of heavy metal pollution on soil microbial community structure and diversity on both sides of a river around a mining area. International Journal of Environmental Research and Public Health, 17(16): 5680, doi: 10.3390/ijerph17165680.

Zhou Y Z, Wang Y, Zeng H, et al. 2015. Spatial heterogeneity and pollution characteristics of heavy metals in Inner Mongolian soils. Journal of Ecology and Environment, 24(8): 1381–1387. (in Chinese)

Appendix

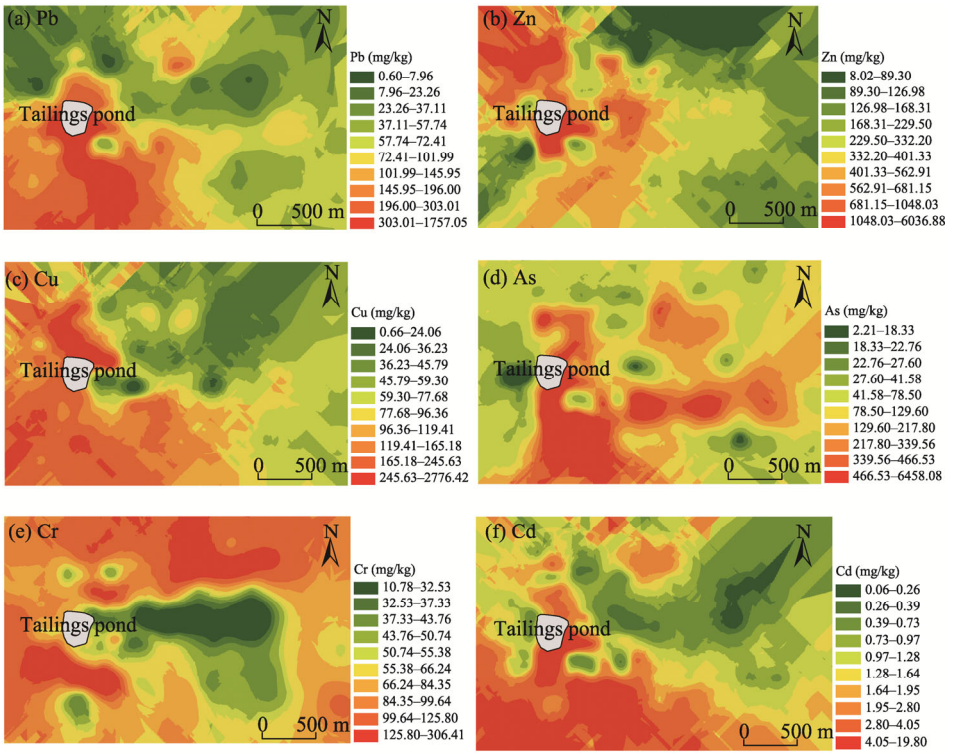

Fig. S1 Spatial distribution of the content of lead (Pb; a), zinc (Zn; b), cuprum (Cu; c), arsenic (As; d), chromium (Cr; e), and cadmium (Cd; f)

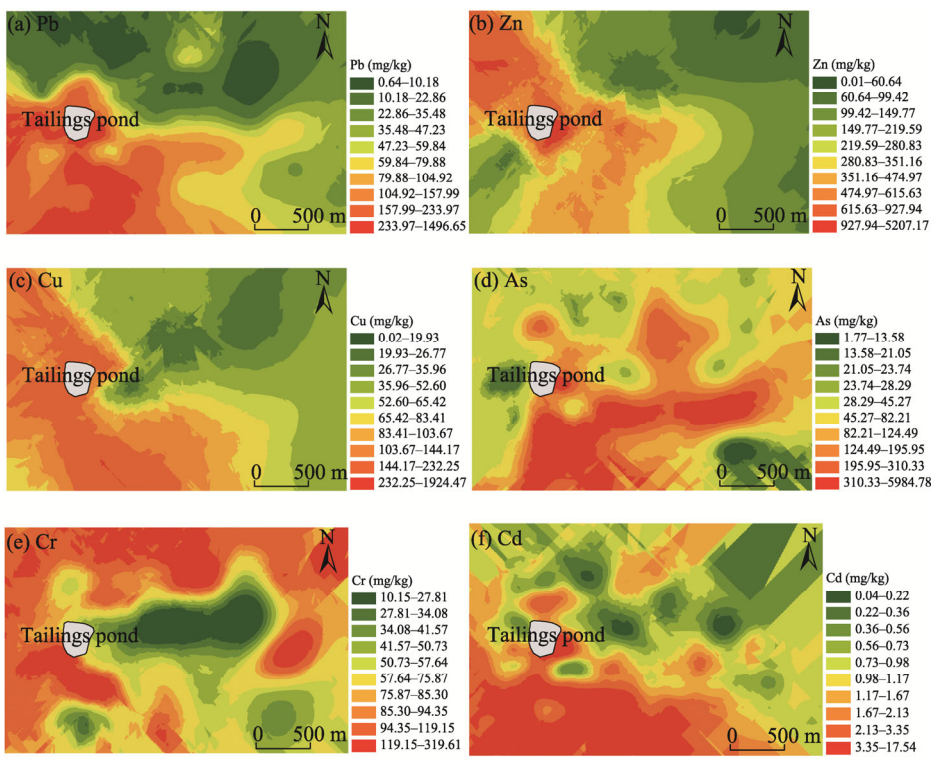

Fig. S2 Spatial distribution of the content of Pb (a), Zn (b), Cu (c), As (d), Cr (e), and Cd (f) at 10–20 cm soil depth

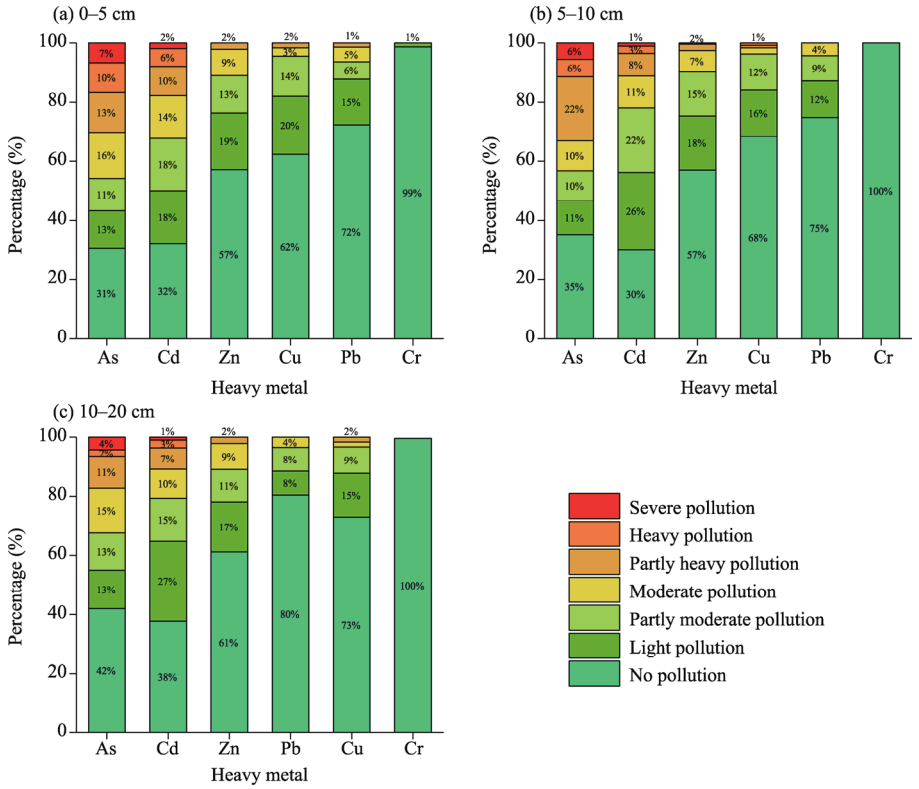

Fig. S3 Percentage of the geo-accumulation index (I_{geo}) at 0–5 (a), 5–10 (b), and 10–20 (c) cm soil depths

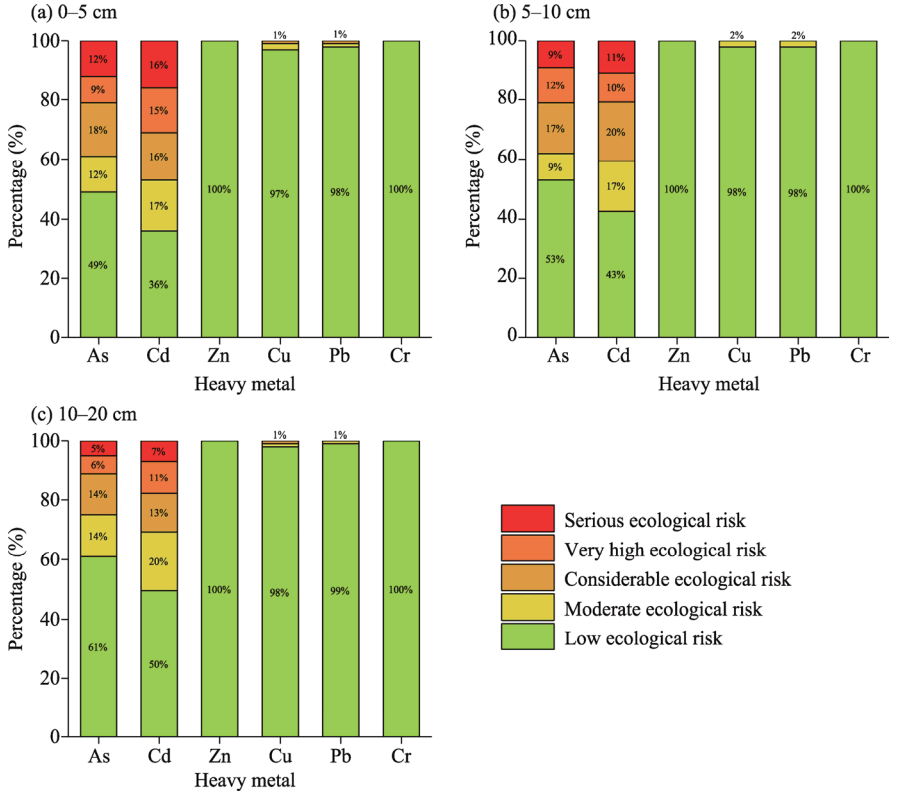

Fig. S4 Percentage of the potential ecological risk factor of a single heavy metal (E_r^i) at 0–5 (a), 5–10 (b), and 10–20 (c) cm soil depths

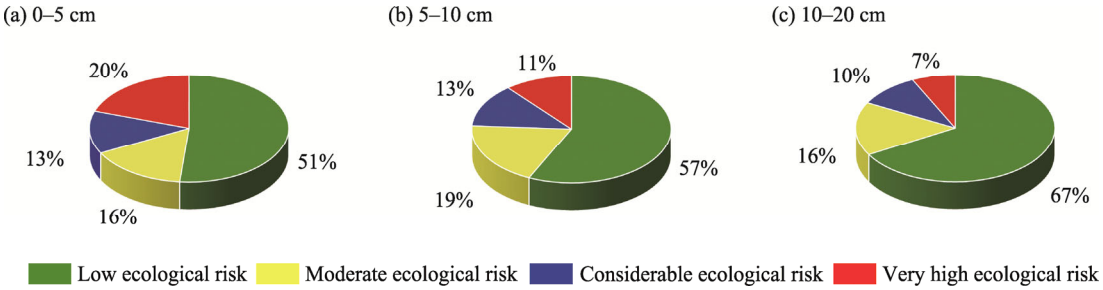

Fig. S5 Percentage of potential ecological risk index (*RI*) at 0–5 (a), 5–10 (b), and 10–20 (c) cm soil depths

Table S1 Statistical analysis results of soil heavy metal content

Soil depth (cm)	Parameter	Cu (mg/kg)	Pb (mg/kg)	Zn (mg/kg)	As (mg/kg)	Cr (mg/kg)	Cd (mg/kg)	pH	EC (μS/cm)	Elevation (m)
0–5	Mean	163	235	671	425	95	4	7.7	415	747
	Median	105	101	366	119	64	2	8.0	213	748
	Minimum	3	0	18	6	9	0	2.5	57	703
	Maximum	1025	2943	5654	8840	462	87	8.5	3098	788
	SD	163	373	841	933	83	8	0.9	482	20
	CV (%)	100	159	125	220	87	187	11.7	116	3
	Exceeding standard rate (%)	53	34	58	78	10	73			
5–10	Mean	162	200	200	354	88	3	7.7	455	747
	Median	86	80	358	105	59	1	7.9	235	748
	Minimum	1	1	8	2	11	0	2.4	37	703
	Maximum	2776	1757	6037	6458	306	20	8.6	2841	788
	SD	258	294	886	741	67	3	1.0	488	20
	CV (%)	159	147	444	209	76	125	12.4	107	3
	Exceeding standard rate (%)	49	29	56	73	6	66			
10–20	Mean	138	168	620	257	91	4	7.6	557	747
	Median	73	70	304	61	62	1	7.9	302	748
	Minimum	0	1	0	2	10	0	2.7	33	703
	Maximum	1924	1497	5207	5985	2015	416	8.8	2713	788
	SD	198	257	828	656	142	30	0.9	546	20
	CV (%)	144	153	134	256	155	722	12.3	98	3
	Exceeding standard rate (%)	41	23	52	64	5	62			

Note: CV, coefficient of variation.

Table S2 Mean value of E_r^i and *RI* of soils at different depths

Soil depth (cm)	E_r^i						*RI*
	Cu	Zn	Cr	As	Cd	Pb	
0–5	10	2	1	160	209	7	388
5–10	9	2	1	132	123	6	273
10–20	8	2	1	95	182	4	291

Note: E_r^i, potential ecological risk factor of single heavy metal; *RI*, potential ecological risk index.